NEOPLASIA
www.neoplasia.com

Volume 12 Number 9 September 2010 pp. 748–754 748

Reactive Astrocytes Protect Melanoma Cells from Chemotherapy by Sequestering Intracellular Calcium through Gap Junction Communication Channels[1]

Qingtang Lin*,[2], Krishnakumar Balasubramanian*,[2], Dominic Fan*, Sun-Jin Kim*, Lixia Guo*, Hua Wang*, Menashe Bar-Eli*, Kenneth D. Aldape† and Isaiah J. Fidler*

*Department of Cancer Biology, The University of Texas MD Anderson Cancer Center, Houston, TX, USA; †Department of Pathology, The University of Texas MD Anderson Cancer Center, Houston, TX, USA

Abstract

Brain metastases are highly resistant to chemotherapy. Metastatic tumor cells are known to exploit the host microenvironment for their growth and survival. We report here that melanoma brain metastases are surrounded and infiltrated by activated astrocytes, and we hypothesized that these astrocytes can play a role similar to their established ability to protect neurons from apoptosis. In coculture experiments, astrocytes, but not fibroblasts, reduced apoptosis in human melanoma cells treated with various chemotherapeutic drugs. This chemoprotective effect was dependent on physical contact and gap junctional communication between astrocytes and tumor cells. Moreover, the protective effect of astrocytes resulted from their sequestering calcium from the cytoplasm of tumor cells. These data suggest that brain tumors can, in principle, harness the neuroprotective effects of reactive astrocytes for their own survival and implicate a heretofore unrecognized mechanism for resistance in brain metastasis that might be of relevance in the clinic.

Neoplasia (2010) 12, 748–754

Introduction

In the United States, up to 40% of cancer patients develop brain metastasis [1]. The top five primary tumors that lead to brain metastasis are lung, breast, melanoma, renal, and colorectal tumors [2]. The median survival duration of untreated patients is 1 to 2 months, and chemotherapy, in conjunction with surgery and radiation therapy, extends survival to only 4 to 6 months [1]. Poor prognosis in these patients is primarily due to chemoresistance [3]. Traditionally, resistance of brain metastasis to chemotherapy has been attributed to the blood-brain barrier (BBB), which prevents toxic substances from reaching the brain parenchyma [4,5]. However, recent studies have revealed that the BBB is not intact in brain metastasis because metastatic tumor cells release vascular permeability factor also known as vascular endothelial growth factor [4,6]. Moreover, more than 70% of brain metastasis cases exhibit enhanced lesions on magnetic resonance imaging due to leakage of contrast agent from blood vessels, thus indicating BBB permeability [7].

The outcome of brain metastasis in patients depends on multiple interactions between tumor cells and the tumor microenvironment, which metastatic cells exploit to their advantage [8,9]. Astrocytes, the predominant cells in the brain maintain homeostasis of the brain microenvironment [10,11]. They transport various nutrients from the circulation to the neurons, participate in neural signal transduction, and buffer the ionic balance of the extracellular matrix [12–15]. Under pathological conditions, such as trauma, ischemia, and neurodegenerative disease, astrocytes became activated, as indicated by the up-regulation of glial fibrillary acidic protein (GFAP) [16]. These reactive astrocytes have been shown to protect neurons from injury induced apoptosis [11,17,18].

Abbreviations: BBB, blood-brain barrier; CBX, carbenoxolone; GFAP, glial fibrillary acidic protein; GFP, green fluorescent protein; GJC, gap junctional communication; 5-FU, 5-fluorouracil; PE, phycoerythrin; RFP, red fluorescent protein

Address all correspondence to: Isaiah J. Fidler, DVM, PhD, or Krishnakumar Balasubramanian, PhD, Department of Cancer Biology, The University of Texas MD Anderson Cancer Center, 1515 Holcombe Blvd, Unit 854, Houston, TX 77030. E-mail: ifidler@mdanderson.org, krishnakumarb@hotmail.com

[1]This work was supported in part by Cancer Center Support Core Grant CA16672 and grant 1U54-CA143837 (I.J.F.) from the National Cancer Institute, National Institutes of Health. Q.L. was supported by a predoctoral fellowship from The Rosalie B. Hite Foundation at the University of Texas MD Anderson Cancer Center.
[2]Q.L. and K.B. share equal first authorship.
Received 26 April 2010; Revised 8 June 2010; Accepted 10 June 2010

DOI 10.1593/neo.10602

These observations raise the intriguing possibility that reactive astrocytes can also protect melanoma cells in brain metastases from cytotoxicity induced by chemotherapeutic drugs. To test this hypothesis, we studied the sensitivity of various melanoma cells to chemotherapeutic agents when cocultured with mouse astrocytes or fibroblasts. We conclude that astrocytes (but not fibroblasts) significantly reduced apoptosis mediated by the chemotherapeutic agents and that the protective effects of astrocytes resulted from their sequestering calcium from the cytoplasm of the tumor cells.

Materials and Methods

Mice

Athymic Ncr-*nu/nu* male mice were purchased from National Cancer Institute–Frederick Cancer Research Facility (Frederick, MD). Animal protocols were approved and supervised by the University of Texas MD Anderson Cancer Center (Houston, TX) Institutional Animal Care and Use Committee.

Mouse Model of Melanoma Brain Metastasis

Human metastatic melanoma cells were introduced into the brain parenchyma of mice through internal carotid artery injection under microscopy as described previously [19]. After mice developed neurological symptoms (e.g., circling), mice were killed, and the brain tissue was harvested for analysis.

Cell Lines, Cell Cultures, and Reagents

The human metastatic melanoma cell lines A375P, DM-4 (from lymph node metastasis specimens) and TXM-13 (from brain metastasis specimens) were all established at the MD Anderson Cancer Center. All melanoma cell lines were recovered from frozen stocks and cultured as previously described [20]. Immortal mouse astrocytes were established in our laboratory [21]. Calcein-AM, Fura-2AM, Fluo-3AM, Hochest 33342, BAPTA-AM, and connexin 43 antibodies were purchased from Invitrogen (Carlsbad, CA). CBX and propidium iodide were purchased from Sigma (St. Louis, MO). GFAP antibodies were purchased from Biocare Medical (Concord, CA). Paclitaxel was purchased from Bristol-Myers Squibb (New York, NY), cisplatin was from SICOR Pharmaceuticals (Irvine, CA), and 5-fluorouracil (5-FU) was from American Pharmaceutical Partners (Schaumburg, IL).

Scanning Electron Microscopy of Tumor Cells and Astrocytes

A375P human melanoma cells and murine astrocytes (1:1 ratio) were plated on sterilized glass coverslips in 24-well plates at a density of 2.4×10^4 cells/well. After 48 hours, the samples were processed as described previously [22].

Chemoprotection Experiment by Flow Cytometry Analysis

Tumor cells were cultured alone or with green fluorescent protein (GFP)–expressing astrocytes at a ratio of 1:1. After being incubated for 72 hours with chemotherapeutic drugs, floating and adherent cells were harvested and fixed with 70% ethanol. The propidium iodide staining procedure was performed as described previously [23]. The fluorescein isothiocyanate (FITC)–propidium iodide protocol was used to separate the GFP-expressing, FITC-positive astrocyte population from FITC-negative tumor cells (Figure 1). This was followed by an analysis of apoptosis in control untreated tumor cells, followed by tumor cells and tumor-astrocyte cocultured samples incubated with chemotherapeutic agents. Apoptotic tumor cells were assessed as the fraction of cells in the sub-G_0 region. Untreated and apoptotic tumor cells were cultured alone and used as controls. Apoptosis in response to chemotherapeutic drugs in astrocytes cultured alone or cocultured with tumor cells was performed as described above for tumor cells. In this case, apoptosis was assessed as the fraction of GFP-positive cells in the sub-G_0 region (Figure 1).

Transwell Experiment

Transwell Boyden Chamber inserts (0.4-μm pore size; Costar, Corning, NY) were seeded with astrocytes (10^5 cells). Tumor cells

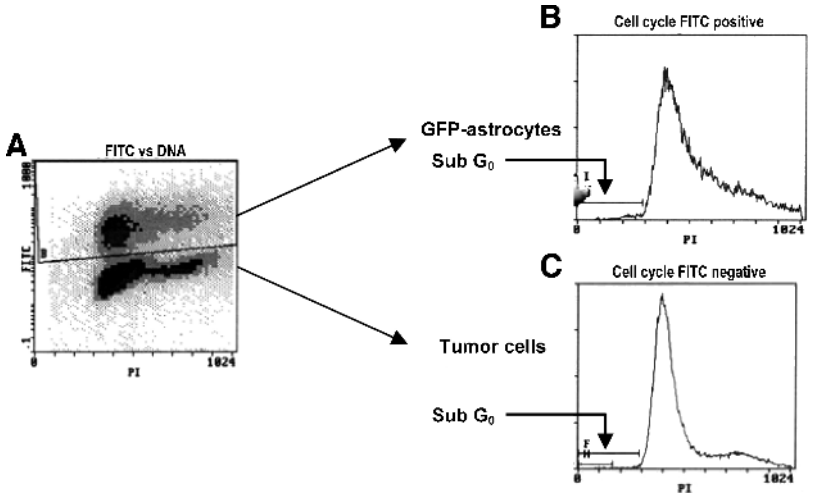

Figure 1. Flow cytometry protocol to analyze the tumor cell death. The FITC–propidium iodide protocol was used to analyze the cell cycle of tumor cells (nonlabeled) and astrocytes (GFP-labeled) separately. The sub-G_0 and -G_1 regions were defined as the percentage of cell death. (A) The GFP gate is able to distinguish tumor cells (bottom) from astrocytes (top). (B) The cell cycle of astrocytes (FITC-positive because of GFP labeling). (C) The cell cycle of tumor cells (FITC-negative).

(10^5 cells) were seeded in the bottom well. Tumor cells were treated with chemotherapeutic drugs and analyzed as described above.

Immunohistochemical Staining

The expression of GFAP and connexin 43 in specimens was analyzed by immunostaining using GFAP (1:50) and Connexin 43 antibodies (1:50) in conjunction with peroxidase (human specimens) or fluorescent (mouse specimens and cell staining) antimouse secondary antibody (1:500). Nuclei were stained using Hochest 33342.

Evaluation of Gap Junctional Communication By Dye Transfer

The dye transfer assay was performed as described previously [24]. In brief, astrocytes (donor cells) were labeled with calcein-AM (5 μM) for 30 minutes at 37°C. Tumor cells (recipient cells) were labeled with DiI (5 μM) for 30 minutes at 37°C. Astrocytes and tumor cells were plated (1:50) in six-well plates. After 6 hours, the cells were harvested and analyzed by fluorescence-activated cell sorting (FACS) to determine the fraction of DiI-positive tumor cells containing calcein.

Knock Down of Connexin 43 in Astrocytes by Short Hairpin RNA

Connexin 43 short hairpin RNA (shRNA; target sequence: shRNA1, –GAAGTTCAAGTACGGGATT– and shRNA 2, –CCATCTTCATCATCTTCAT–) and a nontargeting shRNA (target sequence: TTCTCCGAACGTGTCACGT) were used with the lentiviral system developed and kindly provided by Didier Trono (Ecole Polytechnique Fédérale de Lausanne, Lausanne, Switzerland) as described previously [25].

Western Blot

Total cell extracts (sonification) were separated by gradient (4%-12%) Nu–polyacrylamide gel electrophoresis and transferred to membranes using an iBlot dry blot analysis (Invitrogen). Connexin 43 was detected with antibodies (1:500), using β-actin antibodies (1:3000) as the loading control.

Real-time Polymerase Chain Reaction (Quantitative Polymerase Chain Reaction)

Reverse transcription was performed using the high-capacity RNA-to-cDNA kit (Applied Biosystems, Carlsbad, CA). The gene expression assay for connexin 43 was from Applied Biosystems (assay ID: Mm00439105_m1), with human 18S as the endogenous control (Applied Biosystems). Real-time polymerase chain reaction was performed with the ABI Prism 3000 spectrometer (Applied Biosystems). The relative CT was used for comparison.

Cytoplasmic Calcium Measurement

Temporal analysis of cytosolic Ca^{2+}. At different time intervals, melanoma cells treated with apoptotic agents were labeled with Fura-2AM (1 μM, 30 minutes at 37°C). The cells were then washed and relative changes to cytosolic Ca^{2+} were expressed as the ratio of fluorescence intensities at 340 and 380 nm (λ_{em} = 510 nm) using untreated cells as the control [26].

Flow cytometric analysis of cytosolic Ca^{2+}. A375P melanoma cells were cultured alone or with red fluorescent protein (RFP)–expressing astrocytes. Paclitaxel (10 ng/ml) was added to the culture medium with or without the gap junctional communication (GJC) inhibitor CBX (100 μM). After a 24-hour incubation, the cells were labeled with the Ca^{2+} indicator, Fluo-3AM (2 μM, 30 minutes, 37°C), and washed twice with phosphate-buffered saline. Cytoplasmic Ca^{2+} levels in the harvested cells were determined by flow cytometry using the FITC–phycoerythrin (PE) protocol, which allowed the exclusion of RFP-positive (red) astrocytes from the analysis (Figure 2). Cytoplasmic Ca^{2+} in tumor cells (PE-negative population) was assessed as the mean FITC fluorescence. Data were expressed as the relative change in cytoplasmic calcium compared with control tumor cells that had not been treated with chemotherapeutic agents.

Statistical Analysis

Data are presented as the mean ± SEM. A statistical comparison of treatment sets was performed using the Student's *t* test.

Results and Discussion

In the first set of experiments, we injected human A375 parental cells [20] into the internal carotid artery of nude mice [19]. Mice exhibiting neurological symptoms were killed, and their brain tissue was processed for immunohistological analysis, which revealed that, similar to clinical specimen of human melanoma brain metastases (Figure 3, *A–C*), the experimental melanoma brain metastases (Figure 3, *D–F*) were surrounded and infiltrated by GFAP-positive reactive astrocytes.

In the next set of *in vitro* studies, we used an immortalized astrocyte cell line derived from the brain of *H-2K^b-ts*A58 mice [21] and cocultured these astrocytes with melanoma cells. A scanning electron microscopic examination revealed that the astrocytes formed direct contacts with tumor cells through multiple podia. In some areas, astrocytes and tumor cells formed a seamless structure, which resembled GJC (Figure 3*G*).

Next, we evaluated chemotherapy-induced apoptosis in tumor cells in the absence and presence of astrocytes. Coculture with astrocytes dramatically reduced 5-FU–induced apoptosis in the human melanoma

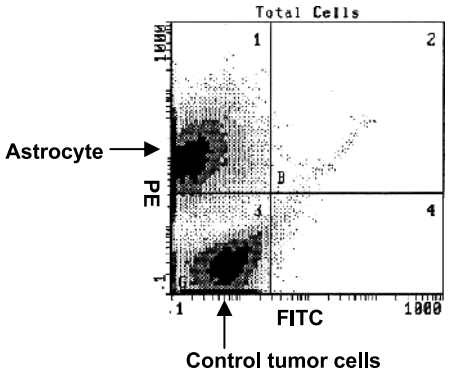

Figure 2. Flow cytometry to analyze the cytoplasmic calcium levels of tumor cells. A375P melanoma cells were cultured alone or with astrocytes (labeled with RFP). Paclitaxel was added to the culture medium, with or without GJC blocker CBX (100 μM). After treatment for 12 hours, calcium indicator Fluo-3AM (2 μM) was added to the medium and incubated for 30 minutes, followed by two washes with phosphate-buffered saline. Cytoplasmic calcium levels were determined by flow cytometry analysis, using the FITC-PE protocol to exclude PE-positive astrocytes.

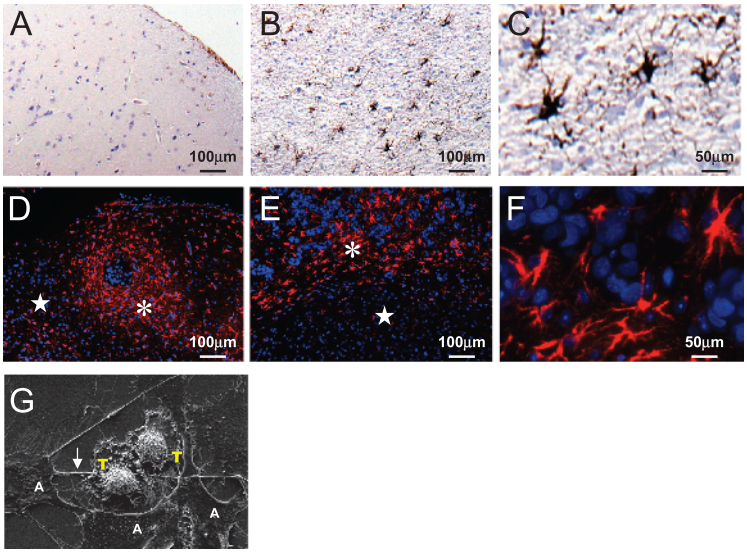

Figure 3. Melanoma-astrocyte interaction. (A–C) A human specimen of melanoma brain metastasis in a tumor free zone (A) shows only sporadic expression of GFAP (brown); in the tumor zone (B), many reactive astrocytes surround and infiltrate tumor lesions; (C) higher magnification of reactive astrocytes in the tumor zone. (D–F) Mouse model of brain metastasis produced by human metastatic melanoma cell lines A375P (D) and TXM13 (E, F). Reactive astrocytes are stained in red, and nuclei are stained in blue. Asterisk (*) indicates tumor zone; star (★), tumor-free zone. (F) Higher magnification of reactive astrocytes from (E). (G) Scanning electron microscopic image of astrocytes (A) and A375P melanoma cells (T) shows direct physical contact between the astrocytes (extending pods-feet) and tumor cells. Note the seamless structure between the astrocytes and tumor cells indicated by the arrowhead.

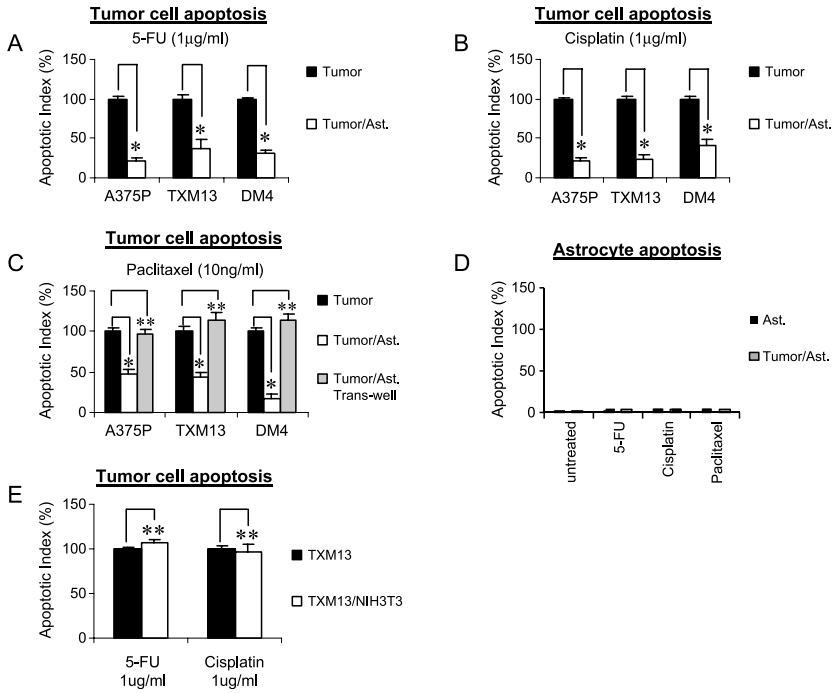

Figure 4. Astrocytes protect melanoma cells from chemotherapy by a mechanism that requires direct physical contact. (A–C) Human melanoma cells were cultured alone or cocultured with GFP-expressing astrocytes (Ast.). After a 72-hour incubation with P-glycoprotein–sensitive (paclitaxel) or –insensitive (5-FU and cisplatin) chemotherapeutic drugs, the cells were harvested and ethanol-fixed, and the apoptotic index of the tumor cells (GFP-negative population) was determined by FACS using the propidium iodide protocol. (C) Physical separation of astrocytes and tumor cells using a transwell membrane (0.4-μm pore size) abolished the protective effect. (D) Astrocytes cultured alone or cocultured with human melanoma cells (TXM13) did not undergo apoptosis after incubation with chemotherapeutic drugs under conditions similar to that described above. (E) Substituting NIH3T3 fibroblasts for astrocytes in (A) and (B) failed to demonstrate protection of tumor cells from chemotherapy. Data are the mean of three experiments. Error bars represent SEM. *$P < .01$, **$P > .05$.

cells A375P, TXM13, and DM-4 by 78.6%, 62.8%, and 69.7%, respectively (Figure 4*A*). This protection was not specific to the chemotherapeutic agent because astrocytes demonstrated similar reductions in cytotoxicity against A375P, TXM13, and DM-4 cells with cisplatin (79.7%, 77.2%, and 59.2%, respectively; Figure 4*B*) and paclitaxel (43.5%, 56.8%, and 82%, respectively; Figure 4*C*). Similar results were also obtained using the MTT cell viability assay [27] (data not shown). Astrocytes cultured alone or cocultured with melanoma cells did not undergo apoptosis when incubated with the chemotherapeutic agents under similar conditions (Figure 4*D*). To determine whether protection by astrocytes required secreted factors or direct physical contact, we repeated the experiments described above but separated the astrocytes from tumor cells by a transwell membrane (0.4-μm pore size). Under these conditions, the astrocytes failed to protect the tumor cells from chemotherapy-induced apoptosis (Figure 4*C*). Substituting murine NIH3T3 fibroblasts for astrocytes in the coculture experiments failed to provide protection (Figure 4*E*). Moreover, because astrocytes protect melanoma cells against both P-glycoprotein–sensitive (paclitaxel) and insensitive (5-FU and cisplatin) drugs [1], the above observations suggest that astrocyte-tumor interactions, rather than P-glycoprotein expression, are a foremost indicator of chemoresistance in melanoma brain metastases [28]. The chemoprotective nature of astrocytes was not restricted to melanoma cells. The protective effect was also demonstrated for human breast cancer cells, human lung cancer cells, and even 3T3 fibroblasts [29].

GJC channels, which directly connect the cytoplasm between adjacent cells, have been shown to be involved in the transmission of survival and apoptotic signals between neighboring cells [30,31]. Both astrocytes and melanoma cells expressed connexin 43, the major GJC at the cell surface (Figure 5*A*). The functionality of GJC was evaluated

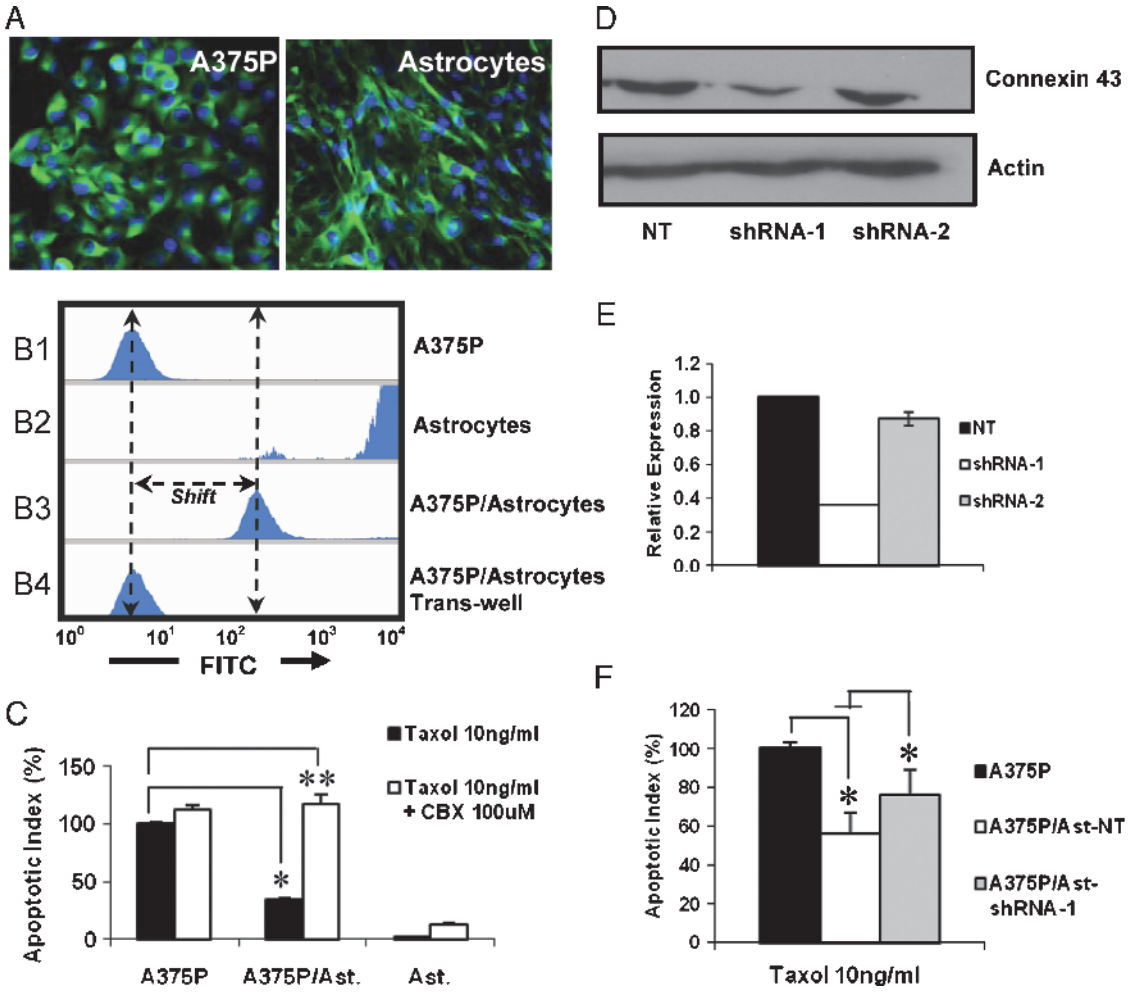

Figure 5. Astrocytes protect melanoma cells through GJC. (A) Expression of connexin 43 in A375P melanoma cells and astrocytes by immunofluorescence staining. (B) Functional assay of GJC. DiI-labeled A375P melanoma cells (B1) and calcein-AM–labeled astrocytes (B2) were coincubated for 6 hours in a CO_2 incubator, followed by FACS analysis (B3). Note that tumor cells are shifted to the right along the FITC axis, indicating the presence of calcein in these cells. The separation of astrocytes and tumor cells by a transwell membrane did not result in calcein-positive tumor cells (B4), underscoring the requirement of direct physical contact for dye transfer. (C) A375P melanoma cells were cultured either alone or together with astrocytes and were incubated for 72 hours with paclitaxel in the absence or presence of the GJC inhibitor, CBX. This was followed by an analysis of the apoptotic index by FACS. Although CBX did not affect apoptosis in single cultures of tumor cells or astrocytes, the inhibitor caused significant reversal of tumor cell protection in the coculture group. (D and E) Western blot analysis (D) and quantitative polymerase chain reaction (E) of connexin 43 expression in astrocytes transduced with lentivirus containing nontargeted (NT) and targeted (shRNA-1 and shRNA-2) sequences. (F) Chemoprotection of tumor cells from paclitaxel-induced apoptosis was partly reversed in Ast-shRNA-1 astrocytes when compared with Ast-NT controls and was determined by coculture experiments. Data are the mean of three experiments. Error bars represent SEM. *$P < .05$.

using the dye transfer assay (Figure 5*B*), which measures the transfer of fluorescent calcein from the astrocytes to the tumor cells; this process can occur only by direct cell-to-cell transfer [30–32]. To determine whether astrocyte-mediated protection of tumor cells occurred through GJC, cocultures were assessed for tumor cell apoptosis in the absence or presence of carbenoxolone (CBX), a specific inhibitor of GJC channels [33,34]. Under these conditions, CBX completely reversed the protection (Figure 5*C*). To confirm the participation of GJC in tumor cell protection, we knocked down expression of connexin 43 in astrocytes [35]. Two shRNA sequences specific against connexin 43 [36] were inserted into lentiviral vectors and transduced into astrocytes. Stable cell lines were established, and the knockdown was confirmed at the protein (Figure 5*D*) and transcription (Figure 5*E*) levels. Analysis of tumor cell apoptosis in coculture experiments with connexin 43–deficient astrocytes (Ast-shRNA-1) revealed increased sensitivity of these tumors to chemotherapy when compared with nontargeted astrocytes (Ast-NT) (Figure 5*F*). Whereas the small interfering RNA approach precludes complete reversal of protection, these data, taken together with the results of the inhibitor experiments (Figure 5, *B* and *C*), underscore the importance of GJC to astrocytes' protection of tumor cells from chemotherapy.

Calcium, one of the most important second messengers transmitted through GJC channels [37], has been shown to play a causal role in cell death [38]. Temporal analysis of melanoma cells incubated with chemotherapeutic agents revealed an increase in cytoplasmic calcium that is followed by the appearance of fragmented DNA, one of the hallmarks of apoptosis (Figure 6*A*). The importance of cytoplasmic calcium to melanoma apoptosis is demonstrated by our finding that its chelation with BAPTA inhibited paclitaxel-induced cell death (Figure 6*B*). Analysis of cytoplasmic Ca^{2+} in paclitaxel-treated tumor cells by flow cytometry revealed that coculture with astrocytes significantly reduced cytoplasmic calcium levels when compared with tumor cells incubated with paclitaxel in the absence of astrocytes (Figure 6*C*). Furthermore, this effect was reversed by the inclusion of the GJC channel blocker CBX in the culture medium (Figure 6*C*). Although we cannot rule out the participation of other molecules by these experiments, these data implicate Ca^{2+} sequestration through GJC channels as a key mechanism by which astrocytes protect the tumor cells from chemotherapy (Figure 6*D*).

Resistance to chemotherapy is one of the major causes of mortality in patients with brain metastasis. Until now, this resistance has been primarily attributed to the impermeable nature of the BBB and the expression of P-glycoprotein by metastatic cells, but we provide here a novel alternate mechanism that requires direct physical connections between activated astrocytes and tumor cells in the brain tumor microenvironment. Taken together, the data presented here underscore the ability of metastatic brain tumors to harness and adopt the neuroprotective properties of resident astrocytes for their own survival. Thus, successful treatment of brain metastasis will require chemotherapy in combination with agents that selectively interfere with the GJC

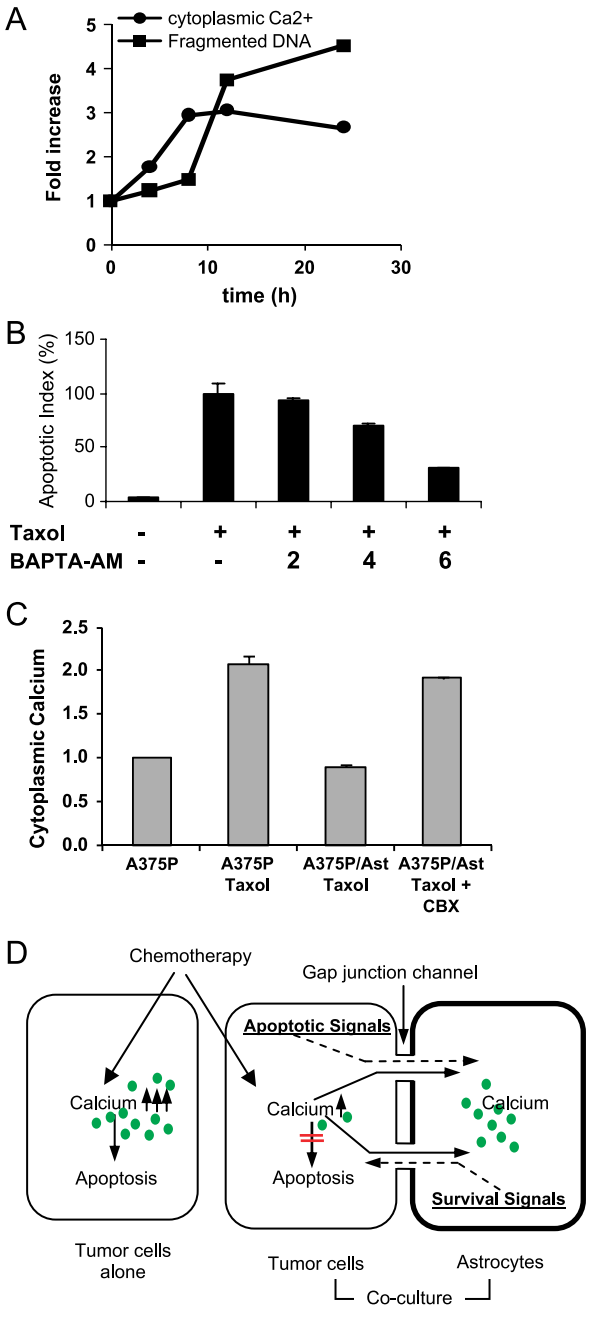

Figure 6. Astrocytes sequester cytoplasmic calcium from tumor cells through GJC. (A) Temporal analysis of cytoplasmic calcium (relative Fura-2 fluorescence) and DNA fragmentation (propidium iodide analysis) in A375P cells incubated with paclitaxel (10 ng/ml). Data are expressed relative to the initial ($t = 0$ hour) values. (B) A375P cells were preincubated with the indicated concentrations of BAPTA-AM before incubation with paclitaxel (10 ng/ml), and the apoptotic index was determined as described earlier. (C) RFP-expressing astrocytes were cocultured with tumor cells and incubated with paclitaxel (10 ng/ml) for 12 hours in the absence or presence of CBX. The cells were then labeled with Fluo-3AM and harvested, and cytoplasmic calcium levels in the tumor cells (RFP-negative) were determined by flow cytometry. Data are presented relative to untreated control tumor cells. Note that inhibition of GJC between tumor cells and the astrocytes with CBX (100 μM) resulted in higher cytoplasmic calcium levels compared with paclitaxel-treated tumor cells alone. (D) Proposed working model for astrocytes' protection of tumor cell apoptosis. When tumor cells cultured alone were treated with chemotherapeutic drugs, an accumulation of cytoplasmic calcium (green circles) led to tumor apoptosis. Coculture of tumor cells with astrocytes, however, resulted in GJC channels between these cells that served as conduits for sequestration and, hence, depletion of calcium and other proapoptotic molecules from the tumor cytoplasm. Alternatively, astrocyte-derived survival factors and signals could be transferred to tumor cells, thereby reducing tumor calcium overload.

channels between these tumor cells and tumor-associated astrocytes. This could potentially be achieved by targeted therapies that are delivered to tumor-associated astrocytes using GFAP antibodies or short nucleotide sequences complementary to GFAP messenger RNA [39].

Acknowledgments

The authors thank Ann Sutton for critical editorial comments and Lola López for expert assistance with the preparation of this article.

References

[1] Soffietti R, Rudā R, and Mutani R (2002). Management of brain metastases. *J Neurol* **249**, 1357–1369.

[2] Schouten LJ, Rutten J, Huveneers HAM, and Twijnstra A (2002). Incidence of brain metastases in a cohort of patients with carcinoma of the breast, colon, kidney, and lung and melanoma. *Cancer* **94**, 2698–2705.

[3] McWilliams RR, Rao RD, Brown PD, Link MJ, and Buckner JC (2005). Treatment options for brain metastases from melanoma. *Exp Rev Anticancer Ther* **5**, 809–820.

[4] Zhang RD, Price JE, Fujimaki T, Bucana CD, and Fidler IJ (1992). Differential permeability of the blood-brain barrier in experimental brain metastases produced by human neoplasms implanted into nude mice. *Am J Pathol* **141**, 1115–1124.

[5] Stewart DJ (1994). A critique of the role of the blood-brain barrier in the chemotherapy of human brain tumors. *J Neurooncol* **20**, 121–139.

[6] JuanYin J, Tracy K, Zhang L, Munasinghe J, Shapiro E, Koretsky A, and Kelly K (2009). Noninvasive imaging of the functional effects of anti-VEGF therapy on tumor cell extravasation and regional blood volume in an experimental brain metastasis model. *Clin Exp Metastasis* **26**, 403–414.

[7] Rowley HA, Scialfa G, Gao PY, Maldjian JA, Hassell D, Kuhn MJ, Wippold FJ II, Gallucci M, Bowen BC, Schmalfuss IM, et al. (2008). Contrast-enhanced MR imaging of brain lesions: a large-scale intra-individual crossover comparison of gadobenate dimeglumine *versus* gadodiamide. *Am J Neuroradiol* **29**, 1684–1691.

[8] Fidler IJ (2003). The pathogenesis of cancer metastasis: the "seed and soil" hypothesis revisited. *Nat Rev Cancer* **3**, 453–458.

[9] Fidler IJ, Yano S, Zhang RD, Fujimaki T, and Bucana CD (2002). The seed and soil hypothesis: vascularisation and brain metastases. *Lancet Oncol* **3**, 53–57.

[10] Abbott NJ, Rönnbäck L, and Hansson E (2006). Astrocyte-endothelial interactions at the blood-brain barrier. *Nat Rev Neurosci* **7**, 41–53.

[11] Sofroniew MV (2005). Reactive astrocytes in neural repair and protection. *Neuroscientist* **11**, 400–407.

[12] Fields RD and Stevens-Graham B (2002). New insights into neuron-glia communication. *Science* **298**, 556–562.

[13] Bullock TH, Bennett MV, Johnston D, Josephson R, Marder E, and Fields RD (2005). Neuroscience: the neuron doctrine, redux. *Science* **310**, 791–793.

[14] Miller G (2005). Neuroscience: the dark side of glia. *Science* **308**, 778–781.

[15] Allen NJ and Barres BA (2009). Neuroscience: glia—more than just brain glue. *Nature* **457**, 675–677.

[16] Crooks DA, Scholtz CL, Vowles G, Greenwald S, and Evans S (1991). The glial reaction in closed head injuries. *Neuropathol Appl Neurobiol* **17**, 407–411.

[17] Mahesh VB, Dhandapani KM, and Brann DW (2006). Role of astrocytes in reproduction and neuroprotection. *Mol Cell Endocrinol* **246**, 1–9.

[18] Chen LW, Yung KL, and Chan YS (2005). Reactive astrocytes as potential manipulation targets in novel cell replacement therapy of Parkinson's disease. *Curr Drug Targets* **6**, 821–833.

[19] Schackert G and Fidler IJ (1988). Development of *in vivo* models for studies of brain metastasis. *Int J Cancer* **41**, 589–954.

[20] Zhang RD, Price JE, Schackert G, Itoh K, and Fidler IJ (1991). Malignant potential of cells isolated from lymph node or brain metastases of melanoma patients and implications for prognosis. *Cancer Res* **51**, 2029–2035.

[21] Langley RR, Fan D, Guo L, Zhang C, Lin Q, Brantley EC, McCarty JH, and Fidler IJ (2009). Generation of an immortalized astrocyte cell line from *H-2K^b-ts*A58 mice to study the role of astrocytes in brain metastasis. *Int J Oncol* **35**, 665–672.

[22] Peng Q, Moan J, Ma LW, and Nesland JM (1995). Uptake, localization, and photodynamic effect of meso-tetra(hydroxyphenyl)porphine and its corresponding chlorin in normal and tumor tissues of mice bearing mammary carcinoma. *Cancer Res* **55**, 2620–2626.

[23] Weihua Z, Tsan R, Huang W-C, Wu Q, Chiu C-H, Fidler IJ, and Hung M-C (2008). Survival of cancer cells is maintained by EGFR independent of its kinase activity. *Cancer Cell* **13**, 385–393.

[24] Fonseca PC, Nihei OK, Savino W, Spray DC, and Alves LA (2006). Flow cytometry analysis of gap junction–mediated cell-cell communication: advantages and pitfalls. *Cytometry* **69**, 487–493.

[25] Villares GJ, Zigler M, Wang H, Melnikova VO, Wu H, Friedman R, Leslie MC, Vivas-Mejia PE, Lopez-Berestein G, Sood AK, et al. (2008). Targeting melanoma growth and metastasis with systemic delivery of liposome-incorporated protease-activated receptor-1 small interfering RNA. *Cancer Res* **68**, 9078–9086.

[26] Balasubramanian K, Mirnikjoo B, and Schroit AJ (2007). Regulated externalization of phosphatidylserine at the cell surface. *J Biol Chem* **282**, 18357–18364.

[27] Meng LH, Zhang H, Hayward L, Takemura H, Shao RG, and Pommier Y (2004). Tetandrine induces early GI arrest in human colon carcinoma cells by downregulating the activity and inducing the degradation of G_1-S–specific cyclin-dependent kinases and by inducing p53 and $p21^{Cip1}$. *Cancer Res* **64**, 9086–9092.

[28] Savas B, Arslan G, Gelen T, Karpuzoglu G, and Ozkaynak C (1999). Multidrug resistant malignant melanoma with intracranial metastasis responding to immunotherapy. *Anticancer Res* **19**, 4413–4420.

[29] Kim SJ, Kim JS, Park ES, Lee JS, Lin Q, Langley RR, Maya M, He J, Kim SW, Weihua Z, et al. (2010). Astrocytes upregulate survival genes in tumor cells and induce protection from chemotherapy. In *Proceeding of the 101st Annual Meeting of the American Association of Cancer Research; April 17–21, 2010; Washington, DC*. Abstract 3428.

[30] Krysko DV, Leybaert L, Vandenabeele P, and D'Herde K (2005). Gap junctions and the propagation of cell survival and cell death signals. *Apoptosis* **10**, 459–469.

[31] Lin JH, Weigel H, Cotrina ML, Liu S, Bueno E, Hansen AJ, Hansen TW, Goldman S, and Nedergaard M (1998). Gap-junction–mediated propagation and amplification of cell injury. *Nat Neurosci* **1**, 494–500.

[32] Blenkinsop TA and Lang EJ (2006). Block of inferior olive gap junctional coupling decreases Purkinje cell complex spike synchrony and rhythmicity. *J Neurosci* **26**, 1739–1748.

[33] Goldberg GS, Moreno AP, Bechberger JF, Hearn SS, Shivers RR, MacPhee DJ, Zhang YC, and Naus CC (1996). Evidence that disruption of connexin particle arrangements in gap junction plaques is associated with inhibition of gap junctional communication by a glycyrrhetinic acid derivative. *Exp Cell Res* **222**, 48–53.

[34] Guan X, Wilson S, Schlender KK, and Ruch RJ (1996). Gap-junction disassembly and connexin 43 dephosphorylation induced by 18 β-glycyrrhetinic acid. *Mol Carcinog* **16**, 157–164.

[35] Rouach N, Avignone E, Même W, Koulakoff A, Venance L, Blomstrand F, and Giaume C (2002). Gap junctions and connexin expression in the normal and pathological central nervous system. *Biol Cell* **94**, 457–475.

[36] Shao Q, Wang H, McLachlan E, Veitch GI, and Laird DW (2005). Downregulation of Cx43 by retroviral delivery of small interfering RNA promotes an aggressive breast cancer cell phenotype. *Cancer Res* **65**, 2705–2711.

[37] Leybaert L, Cabooter L, and Braet K (2004). Calcium signal communication between glial and vascular brain cells. *Acta Neurol Belg* **104**, 51–56.

[38] Roderick HL and Cook SJ (2008). Ca^{2+} signaling checkpoints in cancer: remodeling Ca^{2+} for cancer cell proliferation and survival. *Nat Rev Cancer* **8**, 361–375.

[39] Liu CH, You Z, Ren J, Kim YR, Eikermann-Haerter K, and Liu PK (2008). Noninvasive delivery of gene targeting probes to live brains for transcription MRI. *FASEB J* **22**, 1193–1203.